



Zhao, J., Ghannam, R., Abbasi, Q. , Imran, M. and Heidari, H. (2018)  
Simulation of Photovoltaic Cells in Implantable Application. In: IEEE  
Sensors 2018 Conference, New Delhi, India, 28-31 Oct 2018

This is the author's final accepted version.

There may be differences between this version and the published version.  
You are advised to consult the publisher's version if you wish to cite from  
it.

<http://eprints.gla.ac.uk/166563/>

Deposited on: 04 September 2018

Enlighten – Research publications by members of the University of Glasgow  
<http://eprints.gla.ac.uk>

# Simulation of Photovoltaic Cells for Implantable Sensory Applications

Jinwei Zhao, Rami Ghannam, Qammer H. Abbasi, Muhammad Imran and Hadi Heidari

School of Engineering, University of Glasgow, G12 8QQ, UK

j.zhao.3@research.gla.ac.uk, {Rami.Ghannam, Qammer.Abbasi, Muhammad.Imran, Hadi.Heidari}@glasgow.ac.uk

**Abstract**— Wireless biomedical implantable devices provide a variety of applications based on identification, health, and safety of mankind. Power harvesting and power generation methods through human tissues are still looming challenges because of low efficiency and energy instability. The minimum tissue loss at the optical transparency windows of 650 nm-1350 nm. Photovoltaic cells can be effectively used to provide the necessary power for these implantable devices. However, there have been no previous investigations into the optimum dimensions nor properties of these solar cells. In this case, we show an accurate multi-physics simulation of the performance of photovoltaic cells for implantable devices under the skin. A combination of semiconductor and optical simulations are developed in order to analyse the electro-optic behaviour of these cells. In addition, the efficiencies of 8.97 % and 0.26 % were evaluated under air and air-skin multilayer respectively.

**Keywords**— *Finite element method, implantable, Photovoltaic cell, Power harvesting.*

## I. INTRODUCTION

With the rapid development of biomedical technologies after 21<sup>st</sup> century, health care methods of mankind have been improved in many aspects. Wearable and implantable technologies have been applied in life-science applications, medical diagnosis, and pharmaceutical discovery [1-3]. Related products are tremendously developed such as drug-eluting stents, biosensors and artificial organs [4]. The merging definitions of the internet of things (IoT), self-care and online health monitoring are changing the traditional roles between clients and doctors.

The patients can monitor their health condition at any time with innovative devices, which converts a large scale of data continuously from diagnosing server even located in the different city. In most cases, the reliability and security of implants should be carefully taken into consideration. Moreover, the increasing expectation is proposed for implants to efficiently and continuously communicate with external devices with sufficient and reliable power transducer. There are many topologies to generate or harvest power, such as inductive coupling coils, solar power harvesting, the piezoelectric generator, thermal transducer and electromagnetic power transfer. Firstly, the inductive coils highly depend on the external coil and operating frequency, and it will heat after security or medical scanning in specific workplaces like airport, hospital, and custom. Secondly, the piezoelectric method

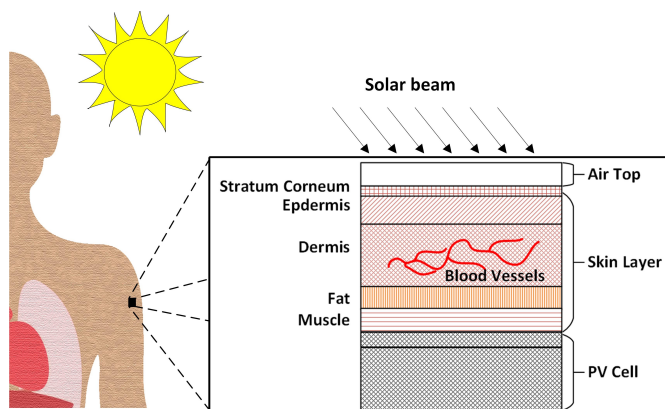


Fig. 1. The multilayer structure of device and ambient.

requires massive motion of muscles and thermal transducers also need to be installed specific location of the body to achieve most differences in temperature. Thirdly, the electromagnetic power transfer is disadvantageous to limited power scale and a huge size. At last, the solar power harvesting is more and more concerned as an implantable power method because of size, independence from the external power provider, microwatts scale output and stability. On the contrary, the solar power harvesting suffers dark condition and operation under the skin. Thus, integrated start-up circuit, maximum power point tracking method (MPPT) and switch-capacitor DC-DC converter attribute to the reliability and rapid response of a solar cell [5, 6].

Modelling and simulation are significant to compare the devices in a range of complex physiological environments [1]. This paper is innovatively the first time to simulate photovoltaic effect and optic physics under the skin to obtain a proper solar cell for the biomedical implantable condition. It must be emphasised that the other researchers involved the industry-fabricated solar cell and validated under the animal skin. However, these devices are not optimized because of different initial purpose [7-8].

## II. PHOTOVOLTAIC EFFECT AND OPTICS ANALYSIS

The photovoltaic (PV) effect was discovered by Edmond Becquerel in 1839 when silver-coated platinum electrodes generated electric power in acid under exposition of sunlight, and it was further explained by Albert Einstein in 1905 [9,10]. Based on this, The PV cell products started in the late 1940s, when silicon photovoltaic product appeared in the industry with

an efficiency of 6 % [11]. It is improved by the development of material and device structure with a goal of maximum power at low cost. The light absorbing material is necessary for all solar cells because the photovoltaic effect makes the formation of electron-hole pairs only if photons can be captured. The photovoltaic effect is the basement to convert the energy between light and electricity [12]. When the light energy is absorbed by cell structure, the electrons and holes are excited, and freely move to conduction band and valence band respectively. To achieve the maximum efficiency of electron-hole pair generation, the incident power of light needs to be controlled slightly greater than the bandgap of the semiconductor. Over-excited electrons are able to acquire higher energy while it will bounce down to bandgap after emitting extra energy via light or heat. After the formation of free electrons, a built-in electric field barrier drives them to produce a current in an external load [11]. For the implantable applications, the situation is even more difficult because of tissue loss and dark condition. The structure of devices and media is shown in Fig. 1. The p-n junction crystalline silicon photodiode is applied in this paper because of the biocompatible material and higher efficiency of the crystalline structure.

With the consideration of solar power issue, it is significant to introduce the light theory which consists of interaction between light and material, electron-hole pair separation in p-n junction as well as the electrical current generation [13]. Since the light intensity is various in the different season, time of day and location. Air Mass 1.5 Global (AM1.5G) is involved as a standard to test the plane solar, which is shown in Fig. 2(d). Air Mass (AM) is defined to describe the different irritation of light.

When solar beams interact with matter, some of them are reflected and refracted, and only parts of beams are absorbed by the device. The absorption, transmission, and reflection are key factors to analyse the optic behaviour inside the devices.

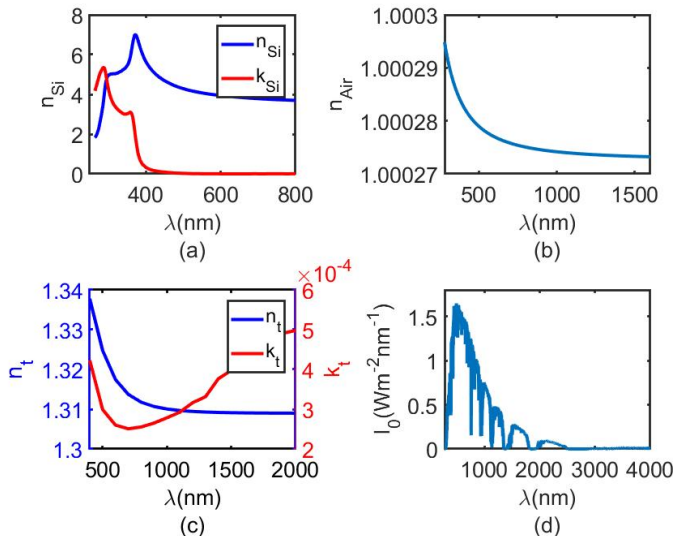


**Fig. 2.** The extracted parameters for COMSOL: (a) the real and imaginary refractive index  $n_{Si}$  and  $k_{Si}$  of silicon (b) the real refractive index of air  $n_{Air}$  (c) the real and imaginary refractive index  $n_t$  and  $k_t$  of skin (d) standard terrestrial spectra of solar light (AM1.5G), and  $\lambda$  is wavelength of incident wave.

The refractive index of air and silicon are shown in Fig. 2(a) and (b) [14,15]. Compared with air and silicon, skin is more complex because of the multilayer structure and variation of gender, age and ethnic. The refractive index of a tissue sample (Caucasian male) is evaluated by absorption coefficient as well as dispersion formula, and it is shown in Fig. 2(c) [16]. Since optic properties of materials are achieved, Jones matrix need to be proposed to analyse optic performance in the multilayer structure, which is shown in Eq. (1) [17]:

$$M_i = \begin{bmatrix} \cos \varphi_i & \left(\frac{i}{\eta_i}\right) \sin \varphi_i \\ i\eta_i \sin \varphi_i & \cos \varphi_i \end{bmatrix} \quad (1)$$

Where  $\varphi_i$  is the phase shift of incident light in the media,  $\eta_i$  is the polarization of incident wave. The reflectance and transmittance of multilayer can be evaluated by the elements of matrix and refractive index of each layer so that the absorption coefficient can be achieved in Eq. (2), which is derivate from [17]:

$$\alpha(\lambda) = \left[\frac{1}{d_i}\right] \ln \left[ \frac{(1-R)^2}{4T} + \frac{\sqrt{(1-R)^4}}{4T^2} + R^2 \right] \quad (2)$$

Where  $d_i$  is the thickness of target layer. It is significant to note that the total absorption coefficient, power flow ( $P_s$ ) and photon flux ( $b_s$ ) highly affects the Generation rate in the semiconductor, which is shown in Eq. (3) [18]. The generation rate demonstrates the quantities of photons which are converted into electrons. In addition, photon flux is related to AM1.5G spectrum.

$$G(x, y, \lambda) = \alpha(x, y, \lambda) b_s(\lambda) P_s(x, y, \lambda) \quad (3)$$

Now turning the point to semiconductor analysis, the doping concentration ( $n$  or  $p$ ) is changing with time along the boundaries of the device. As far as current density ( $J_n$  or  $J_p$ ) is concerned, it highly depends on the generation rate ( $G$ ) and recombination rate ( $U$ ), which is expressed in Eq. (4) and (5) [19]:

$$\frac{\partial n}{\partial t} = \frac{1}{q} \nabla J_n + G - U \quad (4)$$

$$\frac{\partial p}{\partial t} = -\frac{1}{q} \nabla J_p + G - U \quad (5)$$

The recombination rate is composed of Auger, Radiative and Shockley Read Hall recombination, which influences the occupation of holes and lifetime of the electron-hole pairs. In semiconductor design, the longer lifespan is always required to generate the maximum current. The total short circuit current density ( $J_{sc}$ ) can be achieved by integrating the sum of p-n currents with the wavelength. Considering the patristic resistance of a solar cell, the current density-voltage response ( $J$ - $V$ ) can be finally written as Eq. (6) [18]:

$$J(V) = J_{sc} - J_a(V) - \frac{V + J(V)R_s}{R_{sh}} \quad (6)$$

where  $R_s$  and  $R_{sh}$  are series and shunt resistance of solar cell respectively. From the performance of J-V curve, the key

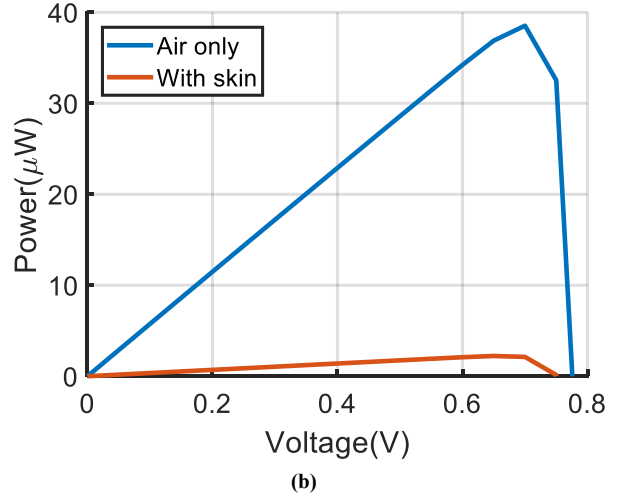
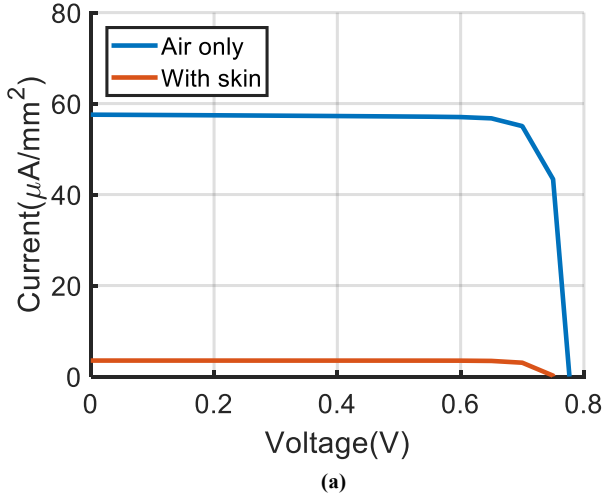


Fig. 3. (a) J-V (current density to Voltage) of the solar cell with air only or skin layer; (b) P-V curve (Power to Voltage) of PV cell.

electric parameters of PV cell such as the output power density ( $P_{max}$ ), open-circuit voltage ( $V_{oc}$ ), filling factor (FF) and the efficiency ( $\eta_{eff}$ ) is achieved.

### III. RESULTS AND DISCUSSION

Fig. 3. (a) and (b) show the J-V curve of 2-dimension (2D) multi-physics simulation made by COMSOL. It is observed that this device provides a short current density ( $J_{sc}$ ) of  $56 \mu A/mm^2$ , an open-circuit voltage ( $V_{oc}$ ) of 0.78 V, a filling factor (FF) of 0.855 and the maximum power ( $P_{max}$ ) of  $38 \mu W$  under air top. It should be noted that the current and power in Fig. 3(a) and (b) should be doubled as  $112 \mu A$  and  $76 \mu W$  respectively because the solar cell is symmetric and only half of the device is simulated. Considering skin loss by Beer-Lambert Law, the short-circuit current is decreased to  $5 \mu A$  (half device) or  $10 \mu A$  (full device), and power is down to  $2.2 \mu W$  (half device) or  $4.4 \mu W$  (full device) in Fig. 3 [18]. To be specific, the skin absorbs most of the power from solar light because the absorptance of air top and skin is much higher than reflectance and transmittance according to Fig. 4. These focused results in transparency window range (650 nm–1350 nm) are simulated by an optic simulator called *Openfilters*. The open-circuit voltage is highly related to the temperature, doping

concentration and the other properties of the semiconductor. However, the doping profile and operating temperature in both simulations are same:  $10^{20} cm^{-3}$  (Acceptor) and  $10^{18} cm^{-3}$  (Donor) with a temperature of 300 K.  $V_{oc}$  shows differences between two simulations because it is also influenced by  $J_{sc}$  and highly affected when band gap is high. The band gap of silicon is 1.12 eV which slightly worsens  $V_{oc}$ . The magnitude of  $J_{sc}$  is related to the area of the device, incident light spectrum, optical performance and collection probability. The area of the device is constantly  $1 mm^2$  and the spectrum is same in Fig. 2 (d). The effect of collection probability can be neglected on ideal contact because the surface passivation disappears, and doping profiles are same. Thus, Optic properties in Fig. 4 are the only factor which makes  $J_{sc}$  decreased. Eventually, the solar cell efficiencies are 8.97 % with air and 0.26 % with skin and air.

### IV. CONCLUSION

A combined optical-electrical Multiphysics model with COMSOL and *OpenFilter* is applied to simulate the performance of silicon p-n junction solar cell based on 2D finite element method. Impressive electric results such as current, voltage, power, efficiency and filling factor are shown. Meanwhile, the optic analysis of skin and air are analysed in *OpenFilter*. The electric performance after involving the skin layer should be also improved because the present power output can only supply few implantable applications. Such drawbacks can be improved by changing junction configuration such as p-i-n structure. In addition, the texture of silicon surface also needs to be considered to improve the light trap and diminish the reflection in surface. The bendability and bio-compatibility will also be concerned to avoid the degradation of device under stress and body rejection. The hybrid power harvester combine with solar and thermal methods will improve the performance of device because they both apply semiconductor material which attributes to better connectivity and wasted heat from solar cell will be recycled by thermal generator.

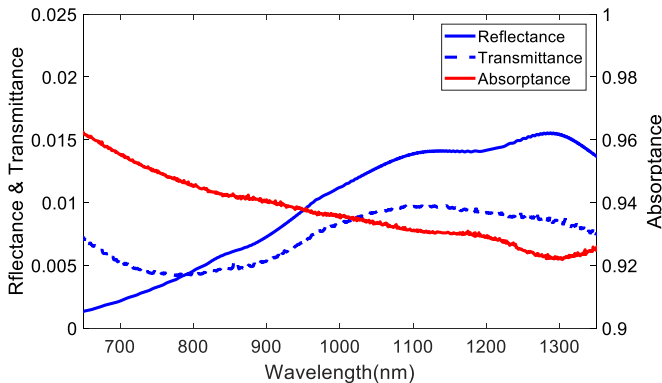


Fig. 4. Reflectance, absorptance and transmittance of multilayer media which contains: air (550nm), human tissue (0.5mm) and silicon PV cell ( $1 \mu m$ ).

## REFERENCES

- [1] V. Nabaei, R. Chandrawati, and H. Heidari, "Magnetic Biosensors: Modelling and Simulation," *Biosens. Bioelectron.*, vol. 103, no. December 2017, pp. 69–86, 2017.
- [2] Z. Yin, E. Bonizzoni, and H. Heidari, "Magnetoresistive Biosensors for On-Chip Detection and Localization of Paramagnetic Particles," *IEEE J. Electromagn. RF Microwaves Med. Biol.*, vol. 2, no. 3, pp. 179–185, 2018.
- [3] H. Heidari, E. Bonizzoni, U. Gatti, and F. Maloberti, "Analysis and modeling of four-folded vertical Hall devices in current domain," in *2014 10th Conference on Ph.D. Research in Microelectronics and Electronics (PRIME)*, 2014, pp. 1–4.
- [4] Y. Onuki, U. Bhardwaj, F. Papadimitrakopoulos, and D. J. Burgess, "A Review of the Biocompatibility of Implantable Devices: Current Challenges to Overcome Foreign Body Response," *J. Diabetes Sci. Technol.*, vol. 2, no. 6, pp. 1003–1015, 2008.
- [5] K. O. Htet, H. Fan, and H. Heidari, "Switched Capacitor DC-DC Converter for Miniaturised Wearable Systems," in *Circuits and Systems (ISCAS), 2018 IEEE International Symposium on*, 2018, pp. 1–5.
- [6] K. O. Htet, R. Ghannam, Q. H. Abbasi, and H. Heidari, "Power Management Using Photovoltaic Cells for Implantable Devices," *IEEE Access*, vol. 6, pp. 42156–42164, 2018.
- [7] Z. Chen, M. K. Law, P. I. Mak, and R. P. Martins, "A Single-Chip Solar Energy Harvesting IC Using Integrated Photodiodes for Biomedical Implant Applications," *IEEE Trans. Biomed. Circuits Syst.*, vol. 11, no. 1, pp. 44–53, 2017.
- [8] S. Ayazian, V. A. Akhavan, E. Soenen, and A. Hassibi, "A photovoltaic-driven and energy-autonomous CMOS implantable sensor," *IEEE Trans. Biomed. Circuits Syst.*, vol. 6, no. 4, pp. 336–343, 2012.
- [9] E. Hecht, *Optics*, 4th ed. Addison-Wesley, 2002.
- [10] M. C. T. Bahaa E. A. Saleh, *Fundamentals of Photonics*, 2nd ed. Wiley-Blackwell, 2001.
- [11] D. M. Chapin, C. S. Fuller, and G. L. Pearson, "A new silicon p-n junction photocell for converting solar radiation into electrical power [3]," *J. Appl. Phys.*, vol. 25, no. 5, pp. 676–677, 1954.
- [12] B. Parida, S. Iniyar, and R. Goic, "A review of solar photovoltaic technologies," *Renew. Sustain. Energy Rev.*, vol. 15, no. 3, pp. 1625–1636, 2011.
- [13] F. Jahanshah, K. Sopian, S. H. Zaidi, M. Y. Othman, N. Amin, and N. Asim, "Modeling the effect of P-N junction depth on the output of planar and rectangular textured solar cells," *Am. J. Appl. Sci.*, vol. 6, no. 4, pp. 667–671, 2009.
- [14] P. E. Ciddor, "Refractive index of air: new equations for the visible and near infrared," *Appl. Opt.*, vol. 35, no. 9, pp. 1566–1573, Mar. 1996.
- [15] "Refractive index." [Online]. Available: <https://refractiveindex.info/?shelf=3d&book=crystals&page=silicon>. [Accessed: 10-Mar-2018]
- [16] T. V. V. Bashkatov A N, Genina E A, "Optical Properties of Skin, Subcutaneous, and Muscle Tissues: a Review," *J. Innov. Opt. Health Sci.*, vol. 4, no. 1, pp. 9–38, 2011.
- [17] S. Larouche and L. Martinu, "OpenFilters: open-source software for the design, optimization, and synthesis of optical filters," *Appl. Opt.*, vol. 47, no. 13, p. C219, 2008.
- [18] X. Li, N. P. Hylton, V. Giannini, K. Lee, N. J. Ekins-Daukes, and S. A. Maier, "Multi-dimensional modeling of solar cells with electromagnetic and carrier transport calculations," *Prog. Photovoltaics Res. Appl.*, vol. 21, no. 1, pp. 109–120, 2013.
- [19] P. P. Altermatt, "Models for numerical device simulations of crystalline silicon solar cells - A review," *J. Comput. Electron.*, vol. 10, no. 3, pp. 314–330, 2011.